Translational Oncology
www.transonc.com

Volume 2 Number 3 September 2009 pp. 121–127 121

Brief Article

Acute Vascular Disruption by 5,6-Dimethylxanthenone-4-Acetic Acid in an Orthotopic Model of Human Head and Neck Cancer[1]

Mukund Seshadri*,† and Karoly Toth*

*Department of Cancer Biology, Roswell Park Cancer Institute, Buffalo, NY 14263, USA; †Department of Preclinical Imaging Facility, Roswell Park Cancer Institute, Buffalo, NY 14263, USA

Abstract

The sustenance of most solid tumors including head and neck cancers (HNCs) is strongly dependent on the presence of a functioning vascular network. In this study, we examined the acute effects of a tumor vascular disrupting agent (VDA), 5,6-dimethylxanthenone-4-acetic acid (DMXAA; ASA404), in an orthotopic model of human HNC. Noninvasive magnetic resonance imaging (MRI) was used to monitor the vascular response of orthotopic FaDu xenografts to VDA therapy. Untreated tumors showed a marked but heterogeneous pattern of enhancement after contrast agent injection on serial T1-weighted (T1W) MR images. After VDA treatment, T2W and T1W MRI revealed evidence of hemorrhaging and lack of functioning vessels (enhancement) within the tumor. Quantitative estimates of relative vascular volume also showed a significant ($P < .01$) reduction in DMXAA-treated tumors 24 hours after therapy compared with untreated controls. Histology and immunostaining of untreated orthotopic FaDu tumors revealed poorly differentiated squamous cell carcinoma histology with distinctly visible $CD31^+$ endothelial cells. In sharp contrast, minimal CD31 staining with irregular endothelial fragments and faint outlines of blood vessels were seen in DMXAA-treated tumor sections. CD31 immunostaining and histology also highlighted the selectivity of vascular damage and tissue necrosis after VDA therapy with no evidence of toxicity observed in normal salivary gland, heart, liver, and skeletal muscle tissues. Together, our results demonstrate a potent and selective vascular disruptive activity of DMXAA in an orthotopic HNC model. Further evaluation into its antitumor effects alone and in combination with other agents is warranted.

Translational Oncology (2009) 2, 121–127

Introduction

Head and neck cancers (HNCs) account for approximately 50,000 new cases of cancer in the United States and result in more than 10,000 deaths [1,2]. Advances in surgical and nonsurgical management have improved response rates in HNC patients, but increases in long-term survival have been modest [3]. Investigation into novel therapies could therefore potentially provide clinical benefit in these patients who often undergo debilitating changes in appearance, speech, and respiratory function after aggressive surgical intervention [3].

Tumor angiogenesis is one of the hallmarks of cancer and a critical determinant of malignant progression of most solid tumors including HNC [4–6]. Early studies carried out in chick chorioallantoic membranes have demonstrated the ability of head and neck tumor cells to induce angiogenesis *in vivo* [7]. A strong association between malignant progression and increased expression of proangiogenic and inflammatory factors has also been demonstrated in HNC [8,9]. On the basis of this knowledge, it was hypothesized that targeting the tumor vasculature could be of potential therapeutic benefit in HNC, particularly in well-vascularized squamous cell carcinomas (SCCs) of the head and neck. To test this hypothesis, in a previous study, the activity of the tumor vascular disrupting agent (VDA), 5,6-dimethylxanthenone-4-acetic acid (DMXAA; ASA404), was investigated against two histologically distinct SCC xenografts implanted subcutaneously in nude mice

Address all correspondence to: Dr. Mukund Seshadri, Department of Cancer Biology, Roswell Park Cancer Institute, Cancer Cell Center 164, Elm and Carlton Streets, Buffalo, NY 14263. E-mail: Mukund.Seshadri@roswellpark.org

[1]This research was supported by the Roswell Alliance Foundation (M.S.) and used core resources supported by the Cancer Center Support Grant by the National Cancer Institute (CA-16056).
Received 14 January 2009; Revised 24 March 2009; Accepted 7 April 2009

DOI 10.1593/tlo.09103

[10]. The results of these studies demonstrated the potent antivascular, antitumor activity of DMXAA against ectopic HNC xenografts [10]. Subcutaneous tumor models are easy to establish, economically feasible, and are useful for rapid screening of therapeutic agents [11]. However, these ectopic tumors do not truly recapitulate the biologic characteristics of human cancers such as angiogenesis and metastatic potential that are influenced by the host microenvironment [11,12]. Particularly with vascular-targeted therapies, it is important to understand the response of tumors within the context of their native tissue environment. Therefore, in this study, the acute effects of DMXAA were investigated in an orthotopic model of human HNC. Changes in vascular function after VDA treatment were monitored using contrast-enhanced magnetic resonance imaging (MRI) in orthotopic FaDu xenografts. Correlative histology and immunohistochemical staining of tumor sections for the endothelial cell adhesion molecule, CD31, was also performed to assess vascular damage after treatment. The results of this study demonstrate, for the first time, potent vascular disruption by DMXAA in an orthotopic model of human HNC.

Materials and Methods

Tumor Model

Eight- to ten-week-old athymic *Foxn1*^{nu} nude mice (Harlan Laboratories, Indianapolis, IN) were fed food and water *ad libitum* and housed in micro isolator cages under ambient light. Orthotopic tumors were established by transcervical injection of 1×10^6 FaDu (human hypopharyngeal SCC) [13] cells into the floor of the mouth of nude mice similar to a procedure previously described by Rosenthal et al. [14]. Experimental studies were performed ~15 to 20 days after implantation in accordance with protocols approved by the Institutional Animal Care and Use Committee.

Vascular Disrupting Agent Treatment

The DMXAA powder (Sigma, St. Louis, MO) was freshly dissolved in D5W (dextrose 5%) and administered to tumor-bearing animals through intraperitoneal injection at a dose of 25 mg/kg, 24 hours before imaging. Untreated control animals did not receive drug or vehicle injection.

Magnetic Resonance Imaging

Tumor-bearing mice were imaged in a 4.7-T/33-cm horizontal bore magnet (GE NMR Instruments, Fremont, CA) incorporating AVANCE digital electronics (Bruker Biospec, ParaVision 3.1.; Bruker Medical, Billerica, MA), a removable gradient coil insert (G060; Bruker Medical) generating a maximum field strength of 950 mT/m, and a custom-designed 35-mm radiofrequency transreceiver coil. Isoflurane (2%-3%; Abbott Laboratories, IL) inhalation was used to induce and maintain anesthesia for imaging. Animals were placed in a prone position on an MR-compatible mouse sled (Dazai Research Instruments, Toronto, Canada) equipped with temperature and respiratory sensors and positioned in the scanner by means of a carrier tube.

T2-weighted (T2W) images were acquired to determine extent of tumor growth and volume using the following parameters: matrix size, 256 × 192; echo time (TE)/repetition time (TR), 40/2424 milliseconds; slice thickness, 1 mm; field of view (FOV), 4.8 × 3.2; number of slices, 21; number of averages, 4; acquisition time, 4 minutes. T1-weighted (T1W) contrast-enhanced MRI using the intravascular contrast agent albumin–gadopentetate dimeglumine (albumin–Gd-DTPA; 0.1 mmol/kg; University of California-San Francisco) was performed in untreated controls and DMXAA-treated animals 24 hours after treatment using a fast spin echo as described previously [10,15]. T1–relaxation rates (R1 = 1/T1) were calculated as an indirect measure of contrast agent concentration in tumor and normal tissues (muscle, brain). Multislice relaxation rate (R1 = 1/T1) maps were obtained using a saturation recovery, fast spin echo scan with variable TR using the following parameters: TE, 10 milliseconds; matrix size, 128 × 96; FOV, 3.2 × 3.2 mm; slice thickness, 1 mm; TR, 360, 500, 750, 1500, 3000, and 6000 milliseconds. For all animals, three baseline images were acquired before contrast agent injection for the estimation

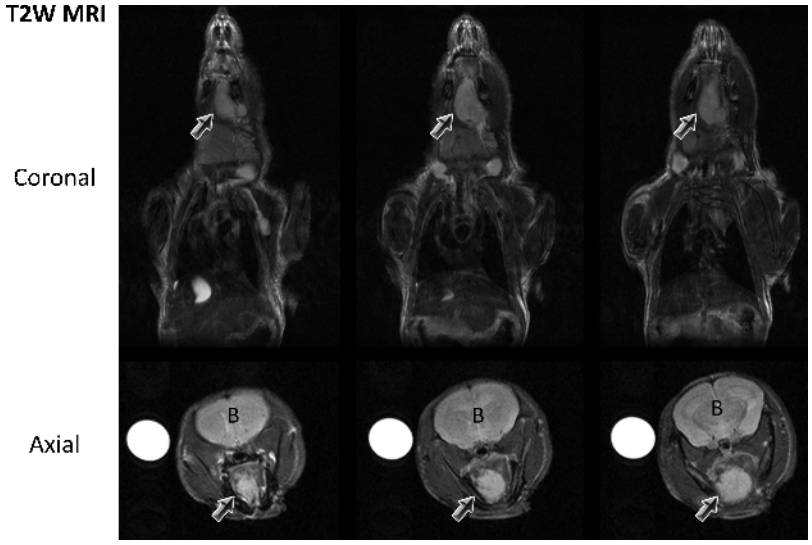

Figure 1. Monitoring growth of orthotopic HNC using MRI. Multislice T2W MR images of a nude mouse acquired on coronal and axial planes showing orthotopic FaDu tumor growth *in vivo*. T2W images provided adequate contrast to allow clear delineation of the tumor from surrounding tissues. *Arrows* indicate tumor; *B*, brain.

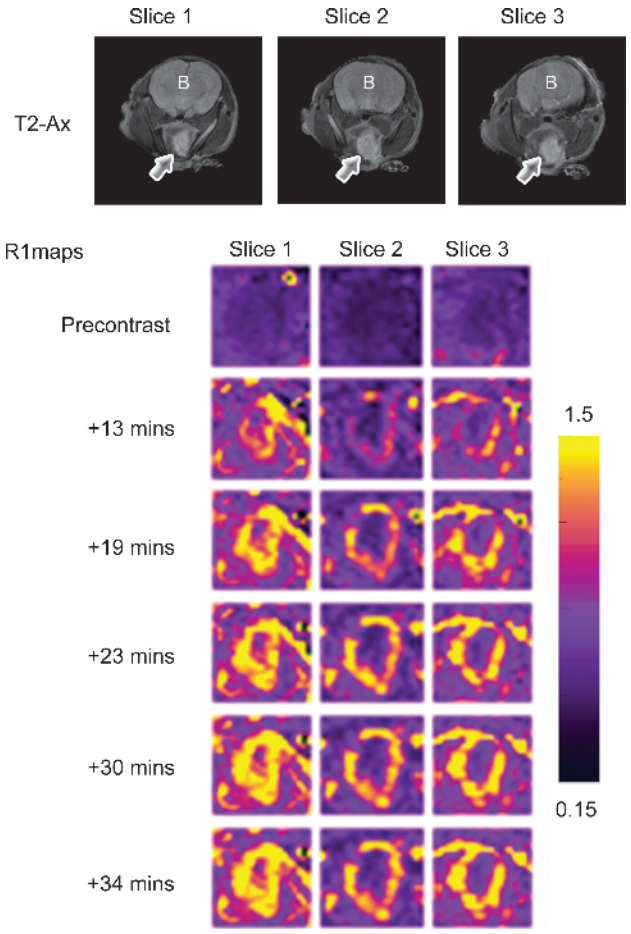

Figure 2. Contrast-enhanced MRI of orthotopic HNC xenografts. Axial T2W images and corresponding pseudocolorized and binarized R1 maps (R1 = 1/T1) of serial slices of an orthotopic FaDu tumor showing a marked but heterogeneous pattern of enhancement during the postcontrast imaging period. The panels of images represent R1 maps calculated on a pixel-by-pixel basis from serial T1W images before (precontrast) and after (post contrast) contrast agent injection for ~40 minutes. *Arrows* indicate tumor; *B*, brain.

of precontrast T1 values. Albumin–$(Gd\text{-}DTPA)_{35}$ was then administrated at a dose of 0.1 mmol/kg as a bolus through tail vein injection, and a series of seven postcontrast images were acquired every 6 minutes for a period of ~45 minutes. Axial images were collected from at least two to three slices through the tumor. Whole-body angiography was acquired using a three-dimensional spoiled gradient recalled echo scan (matrix size, 192 × 96 × 96; FOV, 4.8 × 3.2 × 3.2 cm; TE, 3.0 milliseconds; TR, 15 milliseconds; flip angle, 40°; scan time, = 2 minutes 18 seconds).

After image acquisition, raw image sets were transferred to a workstation for further processing using the medical imaging software, Analyze (AnalyzeDirect, Overland Park, KS). The change in R1 (ΔR1) after contrast agent injection was assumed to be proportional to the tissue concentration of gadolinium. Linear regression analysis of the change in R1 (ΔR1) during the 45-minute postcontrast period time was performed to estimate the relative vascular volume (RVV) of DMXAA-treated and untreated control tumors, and differences were analyzed for statistical significance [10,15]. R1 maps were calculated on a pixel-by-pixel basis using MATLAB (Version 7.0; Mathworks, Inc., Natick, MA) [10,15].

Histology and Immunohistochemistry

Animals from control and treatment groups (n = 3-4 per group) were killed according to Institutional Animal Care and Use Committee guidelines, and tissues were harvested for histology and immunohistochemistry. The tumor, along with adjoining muscle, salivary glands, heart, and liver tissues, was excised to examine the effects of VDA therapy on tumor and normal tissues. Tissue sections were stained for the pan endothelial cell adhesion molecule, CD31, according to previously described procedures [15]. Briefly, excised tissues were placed in zinc fixative for 18 hours and subsequently transferred to 70% ethanol, dehydrated, and embedded in paraffin. Sections 5 μm in thickness were stained with rat anti–mouse CD31 monoclonal antibody (BD Biosciences, San Jose, CA) at 10-μg/ml concentration for 60 minutes at 37°C. Counterstaining of sections was performed with Harris hematoxylin (Poly Scientific, Bay Shore, NY). In place of the primary antibody, an isotype match (rat immunoglobulin G 2a also at 10 μg/ml) was placed on a duplicate slide as a negative control. All slides were read and interpreted by a board-certified pathologist (K.T.).

Glass slides containing various tissue sections were scanned and digitized using the ScanScope XT system (Aperio Technologies, Vista, CA)

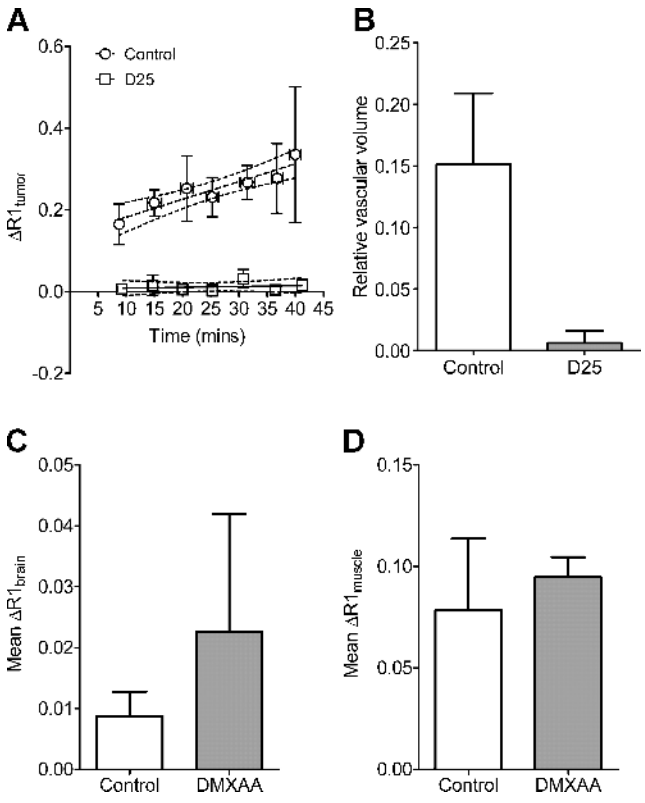

Figure 3. Reduction in vascular volume of orthotopic HNC xenografts after VDA treatment. (A) Temporal change in R1 (ΔR1) values of control and DMXAA-treated orthotopic FaDu tumors calculated during a 40-minute period showing a significant decrease in contrast agent accumulation between control and treatment groups ($P < .001$ between slopes). (B) Calculated RVV of untreated control tumors and DMXAA-treated tumors showed a marked reduction 24 hours after DMXAA treatment compared with untreated controls ($P < .05$), indicative of significant tumor vascular disruption by DMXAA. No significant differences were seen ($P > .5$) in the calculated ΔR1 values of murine brain (C) and muscle tissues (D) from animals in the control and treatment groups.

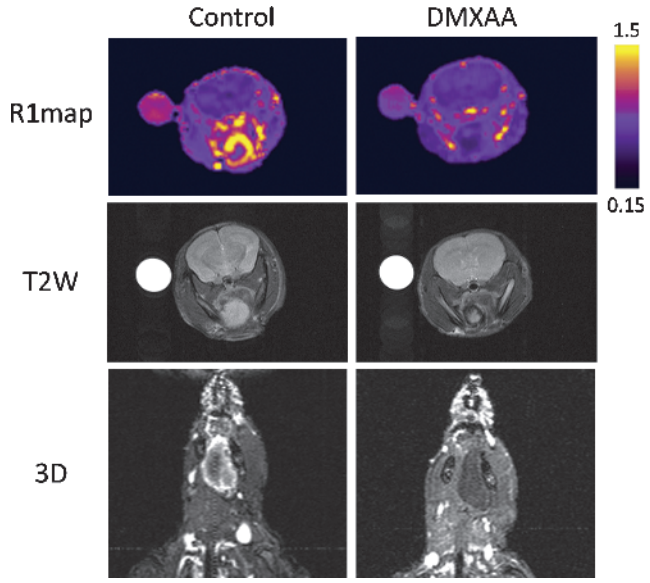

Figure 4. Contrast-enhanced MRI of antivascular therapy in HNC. Pseudocolorized axial R1 maps (top panel), T2W (middle panel), and three-dimensional angiography (bottom panel) of a control mouse (left) and DMXAA-treated mouse (right) 24 hours after treatment. Both R1 maps and three-dimensional images revealed a lack of enhancement within the tumor after contrast in the DMXAA-treated animal compared with untreated control. T2W images of the same animal showed hypointense regions within the tumor 24 hours after treatment, suggestive of hemorrhage.

through the Pathology Resource Network at Roswell Park Cancer Institute. Digitized images were then captured using the ImageScope software (Version 9.1; Aperio Technologies) at a magnification of ×20.

Statistical Analyses

All measured values are reported as mean ± SEM. The 2-tailed *t* test was used to compare ΔR1 values of normal tissues (brain, muscle) of animals between control and treatment groups. $P < .05$ was considered statistically significant. All statistical calculations and analyses were performed using GraphPad Prism (Ver. 5.00 for Windows; GraphPad Software, San Diego, CA).

Results and Discussion

The overall goal of this study was to examine the potential of antivascular therapy in HNC using the tumor VDA, DMXAA. Unlike ectopic tumors established beneath the skin, orthotopic tumors are generally inaccessible to caliper measurement and are often detected by palpation, typically, only during late stages of tumor growth. The use of noninvasive imaging techniques such as MRI is therefore essential for serial (longitudinal) assessment of morphologic and functional changes associated with tumor progression *in vivo*. In the present study, serial anatomic MRI was performed at different times after tumor cell inoculation to visualize the extent and invasion of orthotopic tumor growth *in vivo*. Multislice T2W MR images provided good contrast between tumor and surrounding normal tissues and allowed distinct delineation of the extent of tumor growth *in vivo*. Figure 1 shows coronal and axial T2W MR images of an untreated control mouse bearing orthotopic FaDu tumor (*arrows*) on day 13 after transcervical injection of tumor cells. Tumor volume as measured from the multislice T2W coronal image was 44.6 mm^3. Tumors were established in the floor of the mouth with invasion into the musculature of the tongue during a 3- to 4-week period. Tumor volumes of untreated orthotopic FaDu xenografts measured at different times after implantation were as follows ($n = 5$): day 7 (33.42 ± 8.0), day 14 (46.60 ± 6.3), day 17 (61.64 ± 13.2), and day 24 (83.40 ± 25.6).

Using noninvasive contrast-enhanced MRI, we then examined the perfusion characteristics of orthotopic FaDu tumors before treatment. Contrast-enhanced MRI is a noninvasive technique that provides information pertaining to tumor vascular function based on kinetic analysis of an intravenously administered gadolinium-based contrast agent [16,17]. The methodology is extensively used in preclinical and clinical studies to assess tumor response to antiangiogenic and antivascular therapies [16,17]. Detailed description of the principles and the methodology has been provided by others [16–19]. Using this technique, the pattern of enhancement in control tumors after administration of an intravascular MR contrast agent, albumin–Gd-DTPA [20], was visualized in serially acquired T1W images. Figure 2 shows axial T2W images and corresponding calculated R1 maps of three slices of an orthotopic FaDu tumor before and after contrast agent administration. Axial T2W images provided adequate contrast to allow clear delineation of the tumor margins. R1 maps calculated on a pixel-by-pixel basis before and after contrast agent injection for ~40 minutes showed a marked but heterogeneous pattern of enhancement within the tumor over the postcontrast imaging period (Figure 2; R1 maps).

To assess the acute changes in vascular function after VDA therapy in orthotopic HNC xenografts, T1W contrast-enhanced MRI was performed in a separate cohort of tumor-bearing mice ($n = 4$), 24 hours after treatment with a single injection of DMXAA (25 mg/kg, intraperitoneally) and compared with untreated controls ($n = 4$ per group). The change in longitudinal relaxation rate ($\Delta R1_{tumor}$) was calculated over time in untreated control tumors and DMXAA-treated tumors as an indirect measure of tissue perfusion. As shown in Figure 3*A*, a steady increase in $\Delta R1_{tumor}$ ($r^2 = 0.86$) was observed in untreated control FaDu xenografts highlighting the permeability of vessels to the contrast agent during the 40-minute period. In comparison, 24 hours after treatment, minimal increase in $\Delta R1_{tumor}$ was observed after contrast agent injection ($r^2 = 0.05$, $P < .001$). Linear regression analysis of $\Delta R1_{tumor}$ was then performed to measure the RVV of control and treated tumors based on the change in R1 postcontrast agent injection and precontrast T1 (hence R1) values. Previous studies by others and us have demonstrated that the change in ΔR1 measured over time can be used to RVV (*y*-intercept) and permeability (slope) of tumors [15,18,19]. However, in the present study, linear regression analysis of the temporal change in ΔR1 over time revealed significant differences between the slopes at baseline and posttreatment time points. Therefore, individual estimates of RVV were calculated for each tumor in control and treatment groups and then analyzed for statistical significance using a 2-tailed *t* test. The calculated RVV of control tumors was 0.1513 ± 0.05. In comparison, a marked reduction in RVV (0.0060 ± 0.009, $P < .05$) was observed 24 hours after VDA treatment, indicative of significant tumor vascular disruption by DMXAA. Analysis of ΔR1 values of murine brain (Figure 3*C*) and muscle tissues (Figure 3*D*) did not show any statistical difference between control and treatment groups.

R1 maps were also calculated on a pixel-by-pixel basis to visualize differences in enhancement after contrast agent administration between untreated control tumors and DMXAA-treated tumors. Pseudocolorized and binarized axial R1 maps of a control mouse (*left*) and DMXAA-treated mouse (*right*) are shown in Figure 4. Before treatment,

a marked enhancement was visible within the tumor during the 40-minute period after contrast imaging, indicative of the presence of a functioning vasculature. In contrast, R1 maps of the tumor calculated from images acquired after treatment showed no visible enhancement within the tumor, indicative of treatment-induced reduction in vascular perfusion at the 24-hour time point (*top panel*). T2W images of the same animal also revealed hypointense regions within the tumor, suggestive of hemorrhage compared with the control tumor (*middle panel*). In addition, three-dimensional angiography was performed using a spoiled gradient echo to confirm DMXAA-induced vascular damage *in vivo*. Consistent with the R1 maps, three-dimensional spoiled gradient echo images of the control animal showed considerable enhancement after contrast in the tumor. Corresponding images of the DMXAA-treated animal showed a complete lack of enhancement within the tumor after contrast agent administration confirming tumor vascular response to DMXAA (*lower panel*).

In addition to noninvasive MRI, histology and immunohistochemical staining of tumor sections for the endothelial cell adhesion molecule, CD31, were performed to assess vascular damage after treatment. Consistent with our previous observations with subcutaneous FaDu tumors, orthotopic FaDu xenografts exhibited a poorly differentiated SCC histologic phenotype (Figure 5*A*). CD31-immunostained tumor sections of untreated orthotopic FaDu tumors showed distinctly visible $CD31^+$ endothelial cells (Figure 5*C*). In sharp contrast, hematoxylin and eosin (H&E)–stained sections of treated tumors showed multiple hemorrhagic foci with widespread (>50%) areas of necrosis (Figure 5*B*). Minimal areas of viable tumor cells were visible mostly in the periphery. CD31-immunostained sections of tumors obtained from treated

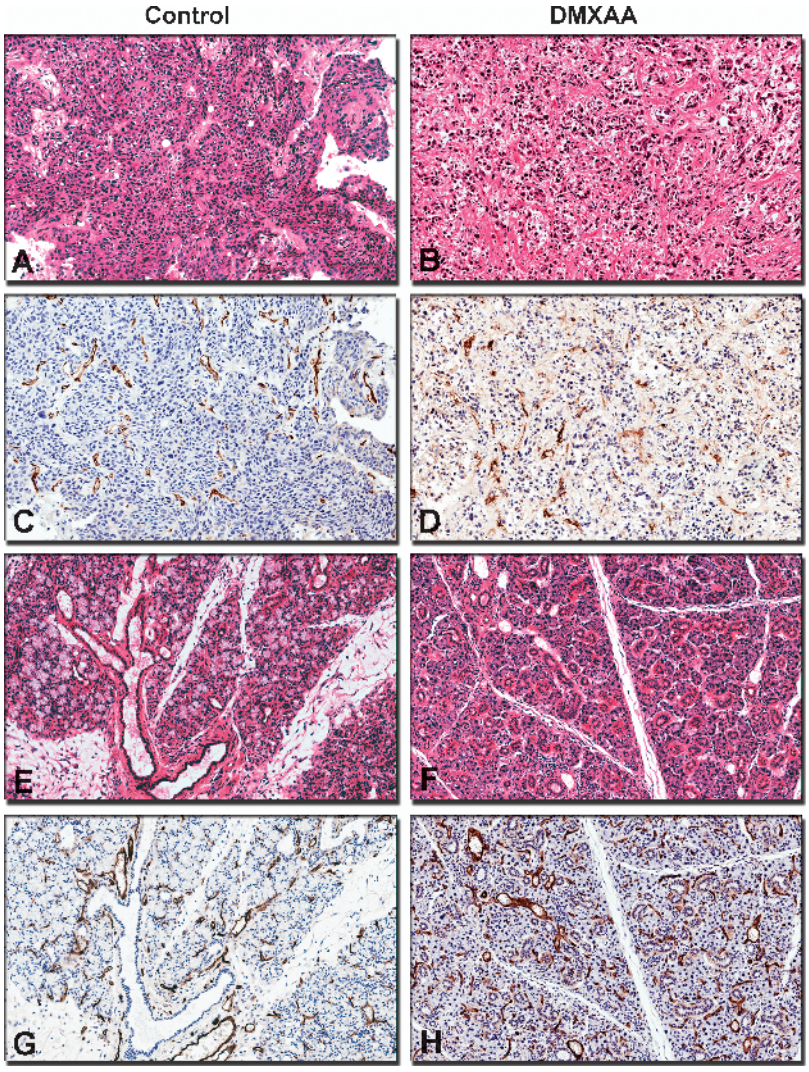

Figure 5. Vascular damage and tumor necrosis after VDA treatment. Panel of digitized images showing tumor (A–D) and normal (E–H) tissue sections obtained from control and DMXAA-treated animals. Control tumors showed a poorly differentiated SCC phenotype (A) and appeared well vascularized with distinctly visible $CD31^+$ endothelial cells (C). In sharp contrast, H&E-stained sections of treated tumors showed widespread areas of necrosis (B). CD31-immunostained sections of tumors obtained from treated animals showed loss of vessel integrity and extensive vascular damage evidenced by minimal or complete absence of CD31 staining (D). H&E-stained sections of salivary glands obtained from both control (E) and treated (F) animals showed normal glandular histology with no tissue necrosis. Corresponding CD31 immunostaining showed no evidence of vascular damage with intact CD31 staining in treated animals (H) similar to controls (G). Digitized images were captured at an apparent magnification of ×20 using the ImageScope software (Version 9.1; Aperio Technologies).

animals showed total loss of vessel integrity and extensive vascular damage evidenced by minimal or complete absence of CD31 staining (Figure 5*D*).

To further investigate the selectivity of the vascular disruptive effects of DMXAA *in vivo*, normal tissues (salivary glands, mouse liver, and heart) were also excised for immunostaining and histology. Salivary glands obtained from both control (Figure 5*E*) and treated (Figure 5*F*) animals showed normal histologic features with intact ductal architecture and viable glandular cells. No evidence of vascular damage was observed in salivary gland tissue with intact CD31 staining in treated animals (Figure 5*H*) similar to controls (Figure 5*G*). CD31 and H&E staining of murine heart and liver tissues also appeared normal with no evidence of vascular damage or tissue necrosis (data not shown).

The vascular disruptive effects of DMXAA have been attributed to a combination of biologic responses ranging from direct drug effects on the endothelium to induction of mediators such as tumor necrosis factor alpha (TNF-α) and serotonin [21]. Although the expression of these mediators was not investigated in the study, we have recently demonstrated increased induction of TNF-α in murine fibrosarcomas after DMXAA treatment [15]. Interestingly, in the previous study, we did not observe any change in TNF levels in murine muscle tissue. Consistent with this previous observation, in the present study, peritumoral skeletal muscle tissue appeared intact with no evidence of vascular damage, further highlighting the selectivity of VDA therapy in the orthotopic HNC model.

Solid tumors are dependent on the presence of a functioning vascular network for their continued growth and differentiation [4,5]. The structural and functional differences between tumor and normal tissue vasculature have led to the development of several agents that result in the selective disruption of tumor-associated blood vessels [22]. These VDAs target existing tumor vessels and have been shown to result in vascular shutdown in a variety of preclinical model systems [22 and references within]. One such tumor-VDA that is currently undergoing active clinical evaluation is DMXAA (ASA404). Phase 1 clinical trials of DMXAA have demonstrated a favorable safety profile of the agent in patients with evidence of pharmacodynamic activity observed at well-tolerated doses [23]. Recent, phase 2 trials of the agent in combination with chemotherapy for lung cancers have also revealed encouraging results [24]. We have previously reported the activity of DMXAA against two ectopic HNC xenografts [10]. The results revealed potent antivascular, antitumor activity of DMXAA against both ectopic HNC xenografts evaluated [10]. However, it is well recognized that the host microenvironment strongly influences the biologic characteristics of tumors including cellular differentiation, angiogenesis, and metastatic potential [11,12]. Therefore, in this study, we examined acute changes in vascular function after DMXAA treatment in orthotopic FaDu HNC xenografts. Although both ectopic and orthotopic FaDu tumors exhibited similar histologic characteristics, an important distinction between tumors established in the two sites lies in their metastatic ability. Experimental studies carried out in our laboratory have shown that orthotopic FaDu tumors exhibit lymph node metastases, whereas subcutaneous tumors do not. This is of particular relevance because head and neck tumors often exhibit locoregional metastases. However, we did not perform a systematic examination of the effect of VDA therapy on nodal metastases, a recognized limitation of the present study. Nevertheless, we have provided a proof-of-principle demonstration of the potent vascular disruptive activity of DMXAA in an orthotopic model of HNC. In addition, our histology/immunohistochemistry results demonstrate the selectivity in the vascular disruptive effects of DMXAA *in vivo* (Figure 5), an issue not entirely addressed our previous study [10].

It is generally believed that VDAs are likely to result in clinical benefit only when used in combination with other therapies. In this regard, we have recently shown that low dose DMXAA potentiates the antitumor efficacy of photodynamic therapy (PDT) against murine colon tumors [25]. Although tumor growth inhibition after VDA monotherapy was not evaluated in the present study, results from our initial studies investigating the long-term response of orthotopic FaDu xenografts to PDT-DMXAA combination therapy have revealed a significant delay in tumor growth after the combination of DMXAA (25 mg/kg) with HPPH-PDT compared with PDT monotherapy (Seshadri, personal communication). The findings of these ongoing studies will be reported as a separate publication focusing on the potential of antivascular therapy (DMXAA) in the combination setting. Ongoing studies are also aimed at performing a systematic evaluation of the activity of DMXAA against patient tumor xenografts established in immunodeficient mice. Successful completion of such preclinical trials of VDAs using surgical tumor specimens obtained from HNC patients would provide a strong rationale and scientific evidence to initiate phase 1 trials of the agent in HNC.

Acknowledgments

The authors thank Robert Brasch and Yanjun Fu (University of California, San Francisco) for providing albumin–Gd-DTPA and Elizabeth Brese and Mary Vaughan at Roswell Park Cancer Institute for their excellent technical assistance.

References

[1] Jemal A, Siegel R, Ward E, Hao Y, Xu J, Murray T, and Thun MJ (2008). Cancer statistics, 2008. *CA Cancer J Clin* **58** (2), 71–96.

[2] Clayman GL, Lippman SM, Laramore GE, and Hong WK (1997). Head and Neck Cancer. In: JF Jolland, E Frei, RC Bast, DW Kufe, DL Morton, and RR Weichselbaum (Eds.), *Cancer Medicine,* 4th ed, Chapter 105. Philadelphia, USA: Williams & Wilkins, pp. 1645–1710.

[3] Conley BA (2006). Treatment of advanced head and neck cancer: what lessons have we learned? *J Clin Oncol* **24**, 1023–1025.

[4] Folkman J (1971). Tumor angiogenesis: therapeutic implications. *N Engl J Med* **285**, 1182–1186; Review.

[5] Hanahan D and Weinberg RA (2000). The hallmarks of cancer. *Cell* **100** (1), 57–70; Review.

[6] Gleich LL, Biddinger PW, Pavelic ZP, and Gluckman JL (1996). Tumor angiogenesis in T1 oral cavity squamous cell carcinoma: role in predicting tumor aggressiveness. *Head Neck* **18**, 343–346.

[7] Petruzzelli GJ, Snyderman CH, Johnson JT, and Myers EN (1993). Angiogenesis induced by head and neck squamous cell carcinoma xenografts in the chick embryo chorioallantoic membrane model. *Ann Otol Rhinol Laryngol* **102** (3 Pt 1), 215–221.

[8] Dunphy F, Stack BC Jr, Boyd JH, Dunleavy TL, Kim HJ, and Dunphy CH (2002). Microvessel density in advanced head and neck squamous cell carcinoma before and after chemotherapy. *Anticancer Res* **22** (3), 1755–1758.

[9] Druzgal CH, Chen Z, Yeh NT, Thomas GR, Ondrey FG, Duffey DC, Vilela RJ, Ende K, McCullagh L, Rudy SF, et al. (2005). A pilot study of longitudinal serum cytokine and angiogenesis factor levels as markers of therapeutic response and survival in patients with head and neck squamous cell carcinoma. *Head Neck* **27** (9), 771–784.

[10] Seshadri M, Mazurchuk R, Spernyak JA, Bhattacharya A, Rustum YM, and Bellnier DA (2006). Activity of the vascular disrupting agent 5,6-dimethylxanthenone-4-acetic acid against human head and neck carcinoma xenografts. *Neoplasia* **8**, 534–542.

[11] Killion JJ, Radinsky R, and Fidler IJ (1999). Orthotopic models are necessary to predict therapy of transplantable tumors in mice. *Cancer Metastasis Rev* **17** (3), 279–284; Review.

[12] Fidler IJ (2001). Angiogenic heterogeneity: regulation of neoplastic angiogenesis by the organ microenvironment. *J Natl Cancer Inst* **93**, 1040–1041.

[13] Rangan SR (1972). A new human cell line (FaDu) from a hypopharyngeal carcinoma. *Cancer* **29** (1), 117–121.

[14] Rosenthal EL, Kulbersh BD, Duncan RD, Zhang W, Magnuson JS, Carroll WR, and Zinn K (2006). *In vivo* detection of head and neck cancer orthotopic xenografts by immunofluorescence. *Laryngoscope* **116**, 1636–1641.

[15] Seshadri M, Bellnier DA, and Cheney RT (2008). Assessment of the early effects of 5,6-dimethylxanthenone-4-acetic acid using macromolecular contrast media–enhanced magnetic resonance imaging: ectopic *versus* orthotopic tumors. *Int J Radiat Oncol Biol Phys* **72** (4), 1198–1207.

[16] Padhani AR and Leach MO (2005). Antivascular cancer treatments: functional assessments by dynamic contrast-enhanced magnetic resonance imaging. *Abdom Imaging* **30**, 324–341.

[17] Hylton N (2006). Dynamic contrast-enhanced magnetic resonance imaging as an imaging biomarker. *J Clin Oncol* **24** (20), 3293–3298.

[18] Brasch R, Pham C, Shames D, Roberts T, Van Dijke K, Van Bruggen N, Mann J, Ostrowitzki S, and Melnyk O (1997). Assessing tumor angiogenesis using macromolecular MR imaging contrast media. *J Magn Reson Imaging* **7** (1), 68–74.

[19] Bhujwalla ZM, Artemov D, Natarajan K, Solaiyappan M, Kollars P, and Kristjansen PE (2003). Reduction of vascular and permeable regions in solid tumors detected by macromolecular contrast magnetic resonance imaging after treatment with antiangiogenic agent TNP-470. *Clin Cancer Res* **9** (1), 355–362.

[20] Ogan M, Schmiedl U, Moseley M, Grodd W, Paajanen H, and Brasch RC (1987). Albumin labeled with Gd-DTPA: an intravascular enhancing agent for magnetic resonance blood pool imaging: preparation and characterization. *Invest Radiol* **22**, 665–671.

[21] Baguley BC (2003). Antivascular therapy of cancer: DMXAA. *Lancet Oncol* **4**, 141–148.

[22] Tozer GM, Kanthou C, and Baguley BC (2005). Disrupting tumour blood vessels. *Nat Rev Cancer* **5**, 423–435.

[23] Li J, Jameson MB, Baguley BC, Pili R, and Baker SD (2008). Population pharmacokinetic-pharmacodynamic model of the vascular disrupting agent 5,6-dimethylxanthenone-4-acetic acid in cancer patients. *Clin Cancer Res* **14** (7), 2102–2110.

[24] McKeage MJ, Von Pawel J, Reck M, Jameson MB, Rosenthal MA, Sullivan R, Gibbs D, Mainwaring PN, Serke M, Lafitte JJ, et al. (2008). Randomised phase II study of ASA404 combined with carboplatin and paclitaxel in previously untreated advanced non–small cell lung cancer. *Br J Cancer* **99** (12), 2006–2012.

[25] Seshadri M and Bellnier DA (2009). The vascular disrupting agent 5,6-dimethylxanthenone-4-acetic acid improves the antitumor efficacy and shortens treatment time associated with photochlor-sensitized photodynamic therapy *in vivo*. *Photochem Photobiol* **85** (1), 50–56.